JOURNAL OF Materials CHEMISTRY

Synthesis and properties of oxygen permeable hydrogels based on copolymers of dimethylacrylamide and fluoro sulfonamide (meth)acrylates

Lisa M. Muratore, Sang Hoon Lee† and Thomas P. Davis

School of Chemical Engineering & Industrial Chemistry, University of New South Wales (UNSW), Sydney, NSW 2052, Australia

Received 1st November 1999, Accepted 25th January 2000

Xerogels have been synthesized from copolymers of dimethylacrylamide and 2-(*N*-alkylperfluorooctanesulfonamido)ethyl (meth)acrylates. The xerogels exhibit transparency despite the fact that DSC analyses reveal heterogeneous structures exhibiting two glass transition temperatures. The DSC results are indicative of a morphology made up of domains corresponding to a rigid backbone and flexible perfluorinated side-chains. On swelling in saline hydrogels were formed. The resulting materials maintain transparency, display high water contents (40–80 wt%) and moduli comparable with existing commercial hydrogel materials. The oxygen permeabilities ($Dk \times 10^{10}$) of the gels range from 34 to 52 (ml O_2) mm cm^{-2} s^{-1} $mmHg^{-1}$. These Dk values are high in comparison with those of conventional hydrogels and are indicative of a heterogeneous hydrogel structure facilitating oxygen transmission through both the aqueous phase and *via* a fluorine-rich co-continuous polymeric phase.

Introduction

The utility of hydrogels as contact lens materials was established by the early work of Wichterle and Lim[1] who described the use of water-swollen crosslinked poly(2-hydroxyethyl methacrylate) (PHEMA) with a water content of around 40 wt%. This discovery spawned a soft contact lens industry and PHEMA is still one of the most popular materials for this application as it is relatively robust, insensitive to small fluctuations in ionic strength and pH and the swollen gel has an oxygen permeability ($Dk \times 10^{10}$ of around 8 (ml O_2) mm cm^{-2} s^{-1} $mmHg^{-1}$. Subsequently an enormous number of patents have been published embracing a large selection of hydrophilic and hydrophobic monomers and different crosslinkers in a range of co- and ter-polymeric formulations. Tighe has published some excellent reviews of the patent literature.[2,3] In conventional hydrogel materials the oxygen transmission is governed by water content and thickness; these two variables can only be optimised at the expense of the physical robustness of the gel. To overcome this limitation, two important strategies have emerged in contact lens material syntheses: namely, the use of silicon- or fluorine-containing materials. In both instances one of the objectives is to increase oxygen permeability of the lens materials. Fluorine incorporation can also imbue other desirable properties to the lens material as it tends to increase the dry hardness of the polymer (improving machinability) whilst also reducing lipophilicity and deposit formation on the lenses in use. One potential drawback to increasing the oxygen permeability by fluorine or silicon incorporation is the accompanying increase in hydrophobicity that ensues; consequently the final polymer is always a compromise of properties. Commercial materials already exist where these synthetic strategies have successfully been adopted for the preparation of hydrogel and/or rigid gas permeable lenses.

A range of fluorine-containing materials have been described in the literature, often involving the copolymerisation of a fluorine-containing monomer with silicon-containing monomers, such as 3-tris[trimethylsiloxysilyl]propyl methacrylate[4] (TRIS) or hydrophilic monomers such as *N*-vinyl-2-pyrrolidone[5] (NVP) or alkylene oxides[6] in random or block sequences. In most instances these strategies have led to hard gas permeable lenses rather than hydrogels. In many of these cases it seems that phase separation occurs in the polymerisation reaction leading to opaque or cloudy compositions of no value for contact lens use. This restricts the compositional range of products that can be made. To overcome this problem hydroxylated fluorine-containing monomers have been suggested to minimise phase separation.[7] Another approach has been described by Mueller[4] who used dimethylacrylamide (DMA) as the hydrophilic monomer and discovered that a wide range of clear fluorine-containing copolymer compositions could be used to fabricate soft contact lenses. In a patent,[4] Mueller claimed the use of fluorine-containing monomers of the structure shown in Fig. 1(a), in conjunction with TRIS and DMA. In our research we have found that fluorine sulfonamide containing acrylic monomers (supplied by 3M), shown in Fig. 1(b), can be copolymerised to yield hydrogel materials with high oxygen permeability, without the addition of TRIS. The purpose of this paper is to describe the syntheses and properties of these materials.

Experimental

Materials

N,*N*-Dimethylacrylamide (DMA) (Sigma-Aldrich Pty. Ltd) was purified by passing over a short column of basic alumina to remove the inhibitor. Fluorinated monomers, 2-(*N*-butylperfluorooctanesulfonamido)ethyl acrylate (FX189), 2-(*N*-ethylperfluorooctanesulfonamido)ethyl acrylate (FX13), and 2-(*N*-ethylperfluorooctanesulfonamido)ethyl methacrylate (FX14), were generously donated by 3M Chemical Co. The structure of these monomers is shown in Fig. 1(b). FX189 was distilled under reduced pressure (bp 130 °C, 10 μmHg) and FX13 and FX14 were both recrystallised twice from ethanol. Ethylene glycol dimethacrylate (EDMA) was purified by column

†*Present address*: Biomedical Laboratory, Korea Institute of Chemical Technology, PO Box 107, Yusung, Taejeon, 30-600, Korea.

DOI: 10.1039/a908656k

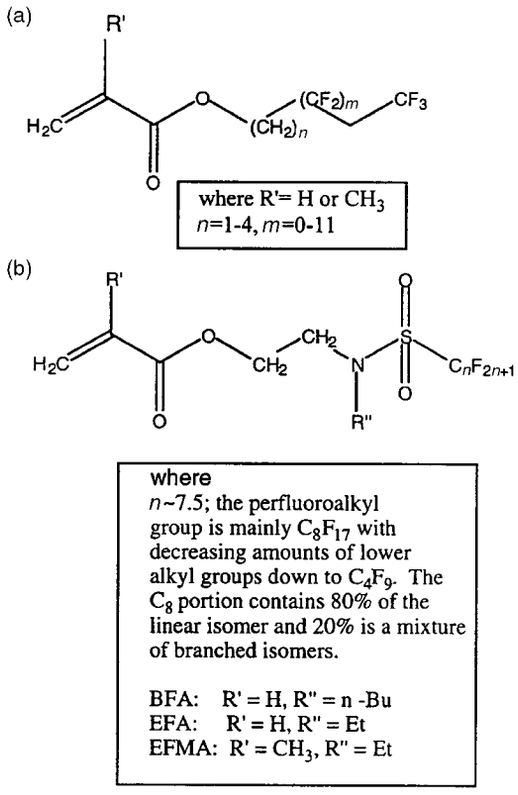

Fig. 1 (a) Structure of fluorine-containing monomers used by Mueller (b) structure of fluorine sulfonamide acrylic monomers.

chromatography using silica gel as absorbent and *n*-hexane–ethyl acetate (7 : 3 v/v) as eluent. Normal (1 M) saline was used for all swelling measurements. We decided to adopt the following abbreviations for the fluorinated monomers: BFA (FX189), EFA (FX13) and EFMA (FX14).

Polymerisation

Monomer mixtures were made up gravimetrically, deoxygenated with nitrogen for 10 min and irradiated in sealed polypropylene ampoules. In all cases the γ-irradiation dose was 1 Mrad obtained from a ^{60}Co source at UNSW, the dose rate being 0.01 Mrad h^{-1} as determined by Fricke dosimetry. The resultant solid rods of xerogel were post-cured at 90 °C for 24 h and then lathe cut to produce thin discs (diameter 10 mm; thickness 1 mm) for swelling measurements, thin discs (diameter 10 mm; thickness 0.1–0.5 mm) for oxygen permeability measurements and cylindrical pellets (diameter 10 mm; thickness 5 mm) for mechanical testing.

In this paper hydrogels are referred to on the basis of the corresponding xerogels. As conversion in these polymerisations is close to 100%, the compositions of xerogels are virtually identical to those of the feed mixtures. The latter are denoted by the weight ratios of components, as described previously.[8–11]

Equilibrium water content

Dimensions of the dry discs and pellets were measured with Vernier calipers and the weighed samples were equilibrated in normal saline at room temperature, the times to attain equilibrium being 2–4 weeks. During this time the saline was changed at frequent intervals to allow for the removal of water-soluble material from the samples.

The equilibrium water content (EWC) of the hydrogels needs to be based on the xerogel weight after sol fraction extraction, in the brine medium

$$\% \text{ sol fraction} = \frac{m_0 - m_E}{m_0} \times 100 \quad (1)$$

where m_E and m_0 represent the dry mass of extracted and unextracted samples respectively. The EWC of the hydrogels is then defined as:

$$EWC = \frac{m_S - m_E}{m_S} \times 100 \quad (2)$$

where m_S = mass of swollen sample. The volume fraction of polymer within a hydrogel is given as

$$\phi_2 = \left(\frac{D_0}{D}\right)^3 \quad (3)$$

where D and D_0 are the diameters of the hydrogel and xerogel respectively.

Oxygen permeability

Measurements were made on swollen samples over a range of thicknesses (at least three) on a JDF Dk1000™ coulometric oxygen permeation instrument under wet cell conditions. The experimental protocol was designed around the method described by Winterton *et al.*[12,13]

Mechanical testing

Elastic moduli of the hydrogels were determined by stress (compression)–strain measurements. The compression rig consisted of a micrometer dial gauge capable of measuring displacement accurately to 0.01 mm. A cylindrical block of Teflon was fastened to the lower end of a shaft that was attached to this gauge. The hydrogel sample was placed centrally on an electronic balance inside a petri dish containing saline solution. The Teflon compressor was moved into contact with the material and the mass recorded as a function of deformation of the sample. The sample was allowed to relax for a least 30 min before re-testing. All samples were tested in triplicate.

Thermal analyses

The glass transition temperatures (T_g) of the xerogels were determined using a TA Instruments DSC 2010 Differential Scanning Calorimeter, at a heating rate of 10 °C min^{-1} using sample weights in the range 5–10 mg. The reported T_g measurements were taken from the second heating run.

Results and discussion

Xerogel synthesis and properties

The xerogel rods were lathe cut into discs (see above); the visual appearance of the discs is shown in Fig. 2(a)–2(c). The polymers containing EFMA, the methacrylate derivative, proved to be either hazy or opaque indicating that this copolymer may be unsuitable for contact lens applications. However, subsequently we discovered that the addition of a crosslinker (1 wt% EDMA, for example) enabled the production of transparent materials. All of the xerogels maintained their transparency on swelling.

In previous work[9,10] the optical homogeneity (or heterogeneity) of xerogels was found to be related to the compositional drift present in the free radical copolymerisation process. Unfortunately reactivity ratios for the copolymerisations described here are not known. However, a qualitative estimation of the extent of compositional drift may be surmised from previous work by Xie and Hogen-Esch[14] who copolymerised DMA with EFA (at low concentrations). Using the Q-e scheme and assuming that EFA is similar in reactivity to methyl acrylate, they estimated reactivity ratios as $r_{DMA} = 1.2$

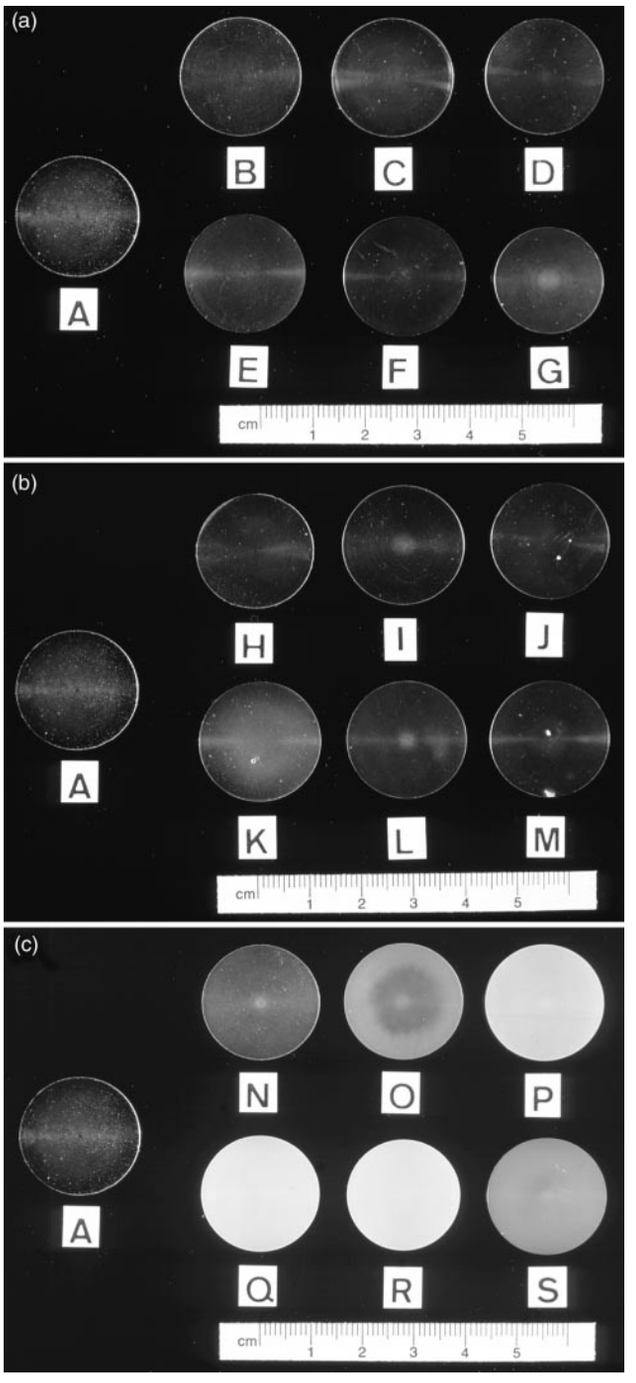

Fig. 2 Photographs of uncrosslinked xerogels where A is DMA homopolymer and (a) B–G are BFA/DMA copolymers containing (sequentially) 10, 20, 30, 40, 50 and 60 wt% BFA, (b) H–M are EFA/DMA copolymers containing (sequentially) 10, 20, 30, 40, 50 and 60 wt% EFA, (c) N–S are EFMA/DMA copolymers containing (sequentially) 10, 20, 30, 40, 50 and 60 wt% EFMA.

and $r_{EFA}=0.6$. These values can be contrasted with the reactivity ratios for DMA with methyl methacrylate (MMA) reported by Liu *et al.*,[15] $r_{DMA}=0.5$, $r_{MMA}=2$. Whilst it is dangerous to overinterpret the applicability of these measurements to our current work it does indicate that the copolymerisation kinetics for systems involving DMA with methacrylates differ significantly from copolymerisations of DMA with acrylates. Therefore the differences in optical appearance of the xerogels may possibly be attributable to compositional drift, and subsequent phase separation between fluorine and non-fluorine rich areas. Further work is required to clarify this issue.

One surprising feature of these copolymer systems is the fact that the transparency is maintained on swelling with water. This is despite the presence of long perfluorinated side-chains which may be expected to aggregate in an aqueous environment, a phenomenon which was exploited by Xie and Hogen-Esch[14] in their work utilising DMA/EFA copolymers as associative thickeners. This suggests that aggregation if it occurs (which seems highly likely) forms domains which are sufficiently small to avoid scattering visible light and/or are virtually isorefractive with the water rich areas.

Finally, we noted that anisotropic swelling sometimes occurred causing deformation of the discs and pellets. The xerogel rods often appeared to contain residual stresses (clearly shown *via* observation between cross-polarising lenses) which we attributed to either inhomogeneities in the original monomer mixing and/or a substantial gel effect which we observed in these reactions. We attempted to solve this problem by placing the monomer mixtures in an ultrasonic bath prior to exposure to the radiation source and by carefully selecting the polymerisation conditions to minimise the gel effect. In the course of this work we found that the dominant cause of the residual stresses was the gel (or Trommsdorf) effect and that by careful control of the polymerisation rate and molecular weight evolution we could ensure the production of samples which would swell isotropically, suitable for lens manufacture. We plan to publish full details of our controlled polymerisation regime in a subsequent publication.

Glass transition temperatures

The T_g values for the xerogels were determined and are shown in Table 1. In all three copolymer systems two T_gs were

Table 1 Glass transition temperatures for uncrosslinked xerogels

Material	Low T_g/°C	High T_g/°C
DMA-100	—	104.1
BFA-20/DMA-80	−8.2	82.7
BFA-40/DMA-60	−9.1	81.8
BFA-60/DMA-40	−13.2	64.6
BFA-100	2.4	—
EFA-20/DMA-80	−2.3	113.7
EFA-40/DMA-60	−16.3	100.2
EFA-60/DMA-40	24.5	71.9
EFMA-20/DMA-80	−14.4	101.9
EFMA-40/DMA-60	−3.2	92.4
EFMA-60/DMA-40	−0.9	80.2

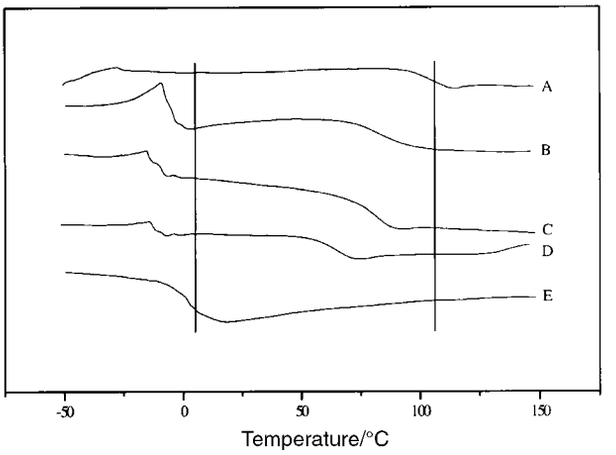

Fig. 3 Thermograms for uncrosslinked BFA/DMA xerogels. The solid vertical lines indicate the T_g values for the two homopolymers where A is DMA homopolymer, B is BFA-20/DMA-80, C is BFA-40/DMA-60, D is BFA-60/DMA-40 and E is BFA homopolymer.

observed. The thermograms for the BFA/DMA series are shown in Fig. 3. The higher T_g is assumed to originate from the DMA component and the lower T_g from the BFA side-chain. Random copolymers usually exhibit only one T_g, given by the weighted average of the T_gs of the two polymeric components. The T_g behaviour observed in the present work is relatively unusual for random copolymers and is normally associated with graft copolymers, where the grafted chain is incompatible with the backbone polymer, or with incompatible polymer blends. Therefore, it seems plausible that the perfluorinated side-chains are sufficiently long and flexible to form domains with a sub-ambient glass transition. The high T_g (corresponding to DMA) is seen to reduce as the concentration of fluoromonomer increases; there is also a concomitant reduction in the lower glass transition. This is concordant with observations previously made by Park *et al.*[16] on graft copolymers of perfluoroalkylethyl methacrylate and methyl methacrylate. The reduction in both T_gs is explicable as follows. The structure of the copolymer is shown in Fig. 4. The high T_g corresponds to the backbone polymer chain region which comprises both DMA and fluoromonomer segments. Thus the high DMA T_g is mediated by a contribution from the fluoromonomer component. The low T_g originates solely from the flexible side-chain most distant from the polymer backbone forming microdomains; this value is lower than the T_g obtained for the pure fluoropolymer as it excludes contributions from the fixed polymer backbone.

Once again, it seems surprising that these copolymers manifest transparency, as it is evident that the materials are inhomogeneous. It may be conjectured that some compatibility may be introduced from two sources. The 'pure' fluoromonomers used in this current study are in fact a mixture of monomers with different length side-chains and thus the extent of incompatibility of the perfluoro side-chains with DMA rich areas may be tempered by a contribution from the smaller side-chains acting as compatibilisers. It is also conceivable that the sulfonamide group in the perfluoro side-chains acts to some extent as a compatibiliser *via* favourable interactions with the tertiary amide group in DMA.

Swelling properties

Uncrosslinked samples. In this work we elected to concentrate our efforts on hydrogels with water contents (EWC) ranging from around 40 to 80 wt% as these materials were predicted to be the most useful as potential soft lenses. Materials with higher water contents were not targeted as we assumed that the tear strengths and moduli would decline. Polymers with lower water contents were ignored as we wished to optimise the hydrophilicity of the materials so that they could be adopted for use as lens materials without any surface treatment. Table 2 shows the swelling data obtained for the three different copolymer systems at selected compositions, prepared in the absence of a crosslinker. As expected the presence of higher fluorine concentrations induces a decrease in the equilibrium swelling. Despite this, it is possible to achieve high water contents whilst maintaining a reasonable fluorine content. This is clearly demonstrated when we compare these new materials with PHEMA with an EWC of about 40 wt%; we can achieve a similar water content with 60 wt% of the fluoromonomers in these new materials. The sol fractions are all fairly low indicating that most of the DMA has copolymerised. It is interesting that the highest sol fractions occur in the hydrogels with the highest DMA concentration; this may indicate the presence of significant compositional drift

Table 2 Swelling properties of uncrosslinked hydrogels at 296 K

Material	EWC/ wt%	ϕ_2	Sol fraction/ wt%
BFA-20/DMA-80	77	0.24	2.4
BFA-40/DMA-60	64	0.37	4.0
BFA-60/DMA-40	42	0.56	1.8
EFA-20/DMA-80	82	0.18	4.6
EFA-40/DMA-60	62	0.34	2.1
EFA-60/DMA-40	41	0.57	1.8
EFMA-20/DMA-80	83	0.17	5.1
EFMA-40/DMA-60	68	0.32	5.7
EFMA-60/DMA-40	50	0.48	3.9

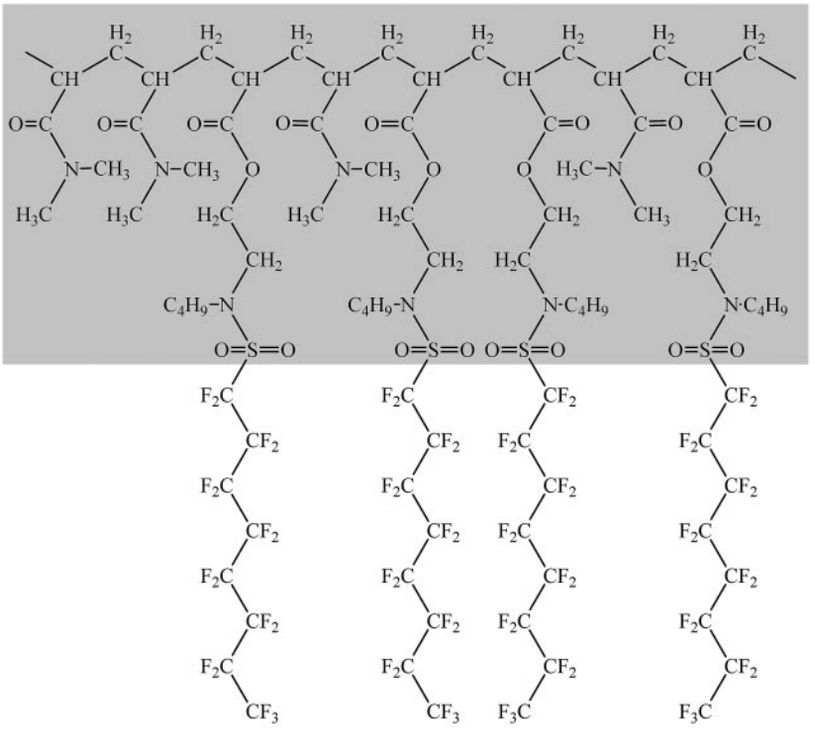

Fig. 4 Structure of BFA/DMA copolymer showing the origin of the two distinct regions giving rise to the two glass transition temperatures.

(as discussed earlier) and the presence of 100% DMA homopolymer. The addition of crosslinking agent at the highest DMA concentrations did little to reduce the sol fraction. This is consistent with previous work,[11] where the reactivity of the crosslinker was shown to be a crucial factor in reducing the sol fraction in hydrogel materials. It should therefore be borne in mind that the final composition (after extraction) of the hydrogels rich in DMA will be slightly different to that designated on the basis of the feed composition. There appear to be no significant differences among the swelling behaviours of the three different copolymer sets.

Crosslinked samples. Table 3 shows the swelling characteristics of the same copolymer systems prepared with 1, 2 and 5 wt% EDMA crosslinker. Increasing concentrations of crosslinker lead to lower EWC values and (generally) lower sol fractions consistent with previous observations made on hydrogel materials.

Oxygen permeability. The oxygen permeabilities obtained on the uncrosslinked hydrogels are given in Table 4. Each reported value is an average of at least three independent measurements. The important factor is the large oxygen permeability of these hydrogel materials compared with non-fluorinated materials. This can clearly be demonstrated if we compare those hydrogels with about 60 wt% fluoromonomer that have water contents around 40 wt% (similar to PHEMA). The oxygen permeability is about five times higher than that of PHEMA. This indicates that oxygen transmission in these hydrogels occurs not only *via* the dissolved oxygen in the aqueous phase but also by another route (which predominates) and which we assume is *via* a co-continuous polymeric phase, which is rich in fluorine. This indicates that the morphology of these gels is an important determinant in the attainment of high oxygen permeability. A further hypothesis leads from this discussion, *viz.* that the water plays two important roles in these materials, first as a direct source of oxygen flux *via* dissolved oxygen (as with conventional hydrogel materials) and secondly by inducing a co-continuous hydrophobic network (*via* hydrophobic interactions) which provides a secondary mechanism for oxygen transmission. The slight rise in oxygen permeability that occurs when the DMA content (and hence the water content) is raised may simply result from the increased contribution to the oxygen flux from water-dissolved oxygen. If this is the case then it indicates that the secondary transmission route (*via* a fluorine rich network) is maintained despite a reduction in the overall fluorine content of the gel. Alternatively, it may indicate that increased ordering of the hydrophobic regions compensates for a loss of oxygen transmission caused by the reduction in fluorine content. Clearly, further morphological studies are required to test some of these ideas.

Table 3 Swelling properties of crosslinked hydrogels at 296 K

Material	EWC/ wt%	ϕ_2	Sol fraction/ wt%
1 wt% EDMA			
BFA-20/DMA-80/EDMA-1	71	0.28	6.9
BFA-40/DMA-60/EDMA-1	55	0.40	1.6
BFA-60/DMA-40/EDMA-1	37	0.60	1.0
EFA-20/DMA-80/EDMA-1	66	0.31	2.2
EFA-40/DMA-60/EDMA-1	52	0.44	1.5
EFA-60/DMA-40/EDMA-1	34	0.64	0.9
EFMA-20/DMA-80/EDMA-1	72	0.26	2.8
EFMA-40/DMA-60/EDMA-1	57	0.39	3.0
EFMA-60/DMA-40/EDMA-1	43	0.53	2.9
2 wt% EDMA			
BFA-20/DMA-80/EDMA-2	64	0.39	12.0
BFA-40/DMA-60/EDMA-2	51	0.48	2.7
BFA-60/DMA-40/EDMA-2	34	0.66	4.1
EFA-20/DMA-80/EDMA-2	64	0.39	8.8
EFA-40/DMA-60/EDMA-2	51	0.51	4.9
EFA-60/DMA-40/EDMA-2	34	0.67	2.6
EFMA-20/DMA-80/EDMA-2	63	0.37	5.8
EFMA-40/DMA-60/EDMA-2	54	0.47	4.9
EFMA-60/DMA-40/EDMA-2	31	0.65	1.8
5 wt% EDMA			
BFA-20/DMA-80/EDMA-5	52	0.47	8.7
BFA-40/DMA-60/EDMA-5	39	0.61	5.0
BFA-60/DMA-40/EDMA-5	29	0.72	4.6
EFA-20/DMA-80/EDMA-5	57	0.47	11.6
EFA-40/DMA-60/EDMA-5	42	0.56	2.7
EFA-60/DMA-40/EDMA-5	28	0.72	2.4
EFMA-20/DMA-80/EDMA-5	56	0.42	5.5
EFMA-40/DMA-60/EDMA-5	40	0.57	4.0
EFMA-60/DMA-40/EDMA-5	25	0.70	2.6

Table 4 Oxygen permeabilities of uncrosslinked hydrogels

Material	$Dk \times 10^{10}$/(ml O_2) mm cm^{-2} s^{-1} $mmHg^{-1}$
BFA-20/DMA-80	47(±6)
BFA-40/DMA-60	44(±2)
BFA-60/DMA-40	41(±7)
EFA-20/DMA-80	51(±3)
EFA-40/DMA-60	43(±5)
EFA-60/DMA-40	34(±6)
EFMA-20/DMA-80	52(±4)
EFMA-40/DMA-60	43(±7)
EFMA-60/DMA-40	47(±18)

Network parameters. Young's moduli, E, were obtained from the slopes in plots of stress (τ) *vs.* strain ($\lambda-1$), where τ is the applied force per unit area of hydrogel and λ is the ratio of the strained to unstrained lengths of the hydrogel.

The effective crosslink density, v_e, was obtained from compression–strain results *via* eqns. (4) and (5):

$$\tau = G\left(\lambda - \frac{1}{\lambda^2}\right) \quad (4)$$

$$G = RTv_e\phi_2^{1/3} \quad (5)$$

where τ is the force/cross-sectional area, R the gas constant, T the absolute temperature and v_e the effective crosslink density (mol m^{-3}).

Values of the polymer–water interaction parameter, χ, were calculated from the following expression valid at swelling equilibrium:

$$\ln(1-\phi_2) + \phi_2 + \chi\phi_2^2 + v_e V_1(\phi_2^{1/3} - 2\phi_2 f^{-1}) = 0 \quad (6)$$

where f = crosslinking functionality of crosslinking agent and V_1 = molar volume of water (dm^3 mol^{-1}).

From the values of v_e the molar mass per crosslink, M_c, was calculated *via*:

$$M_c = \rho / v_e \quad (7)$$

where ρ is the density of the xerogel, calculated from direct weighings and micrometrically measured dimensions of all the dried discs and pellets used.

Table 5 Mechanical properties and derived network parameters for uncrosslinked hydrogels at 296 K

Material	E/MPa	G/MPa	v_e/mol m^{-3}	M_c/kg mol^{-1}	χ
BFA-20/DMA-80	0.10	0.03	21	55	0.59
BFA-40/DMA-60	0.25	0.08	45	28	0.66
BFA-60/DMA-40	0.39	0.12	57	23	0.83
EFA-20/DMA-80	0.09	0.03	21	58	0.57
EFA-40/DMA-60	0.40	0.12	71	18	0.65
EFA-60/DMA-40	0.50	0.15	74	18	0.84
EFMA-20/DMA-80	0.09	0.03	20	58	0.56
EFMA-40/DMA-60	0.14	0.05	30	42	0.64
EFMA-60/DMA-40	0.40	0.13	67	21	0.75

Uncrosslinked hydrogels. The mechanical properties and derived network parameters for the uncrosslinked hydrogels are given in Table 5. There are no significant differences among the three fluoromonomer systems and the moduli increase with decreasing water content (decreasing DMA concentration) as expected. This is consistent with hydrophobic bonding acting as effective crosslinks in these hydrogels.

Crosslinked hydrogels. The mechanical properties and derived network parameters for the crosslinked hydrogels are given in Table 6. From the gravimetric compositions of the xerogels and their densities the theoretical concentrations of crosslinkers (v_t) were calculated. Over the range of EDMA contents used v_e exceeded v_t. A linear dependence of v_e on v_t has been noted previously in hydrogels and a similar empirical relationship was found to hold for two copolymer systems in the present work, as shown in Fig. 5. The slopes and intercepts are recorded in Table 7, where it is evident that the crosslinking is relatively inefficient as evidenced by the low gradients. The intercept values increase with increasing fluoromonomer content as expected.

Conclusion

Materials have been developed that are suitable for use as contact lenses. In the dry state these materials are easily turned on a lathe to produce xerogels which can subsequently be swollen into hydrogels. The main drawback with this approach is the influence of a substantial gel effect, which can induce residual stresses in the xerogels leading to anisotropic swelling. However, a careful polymerisation regime can be adopted to minimise this problem and this will be the subject of a subsequent communication. The hydrogel materials exhibit

Table 6 Mechanical properties and derived network parameters for crosslinked hydrogels at 296 K

Material	E/MPa	G/MPa	v_e/mol m^{-3}	M_c/kg mol^{-1}	χ
1 wt% EDMA					
BFA-20/DMA-80/EDMA-1	0.17	0.05	33	38	0.62
BFA-40/DMA-60/EDMA-1	0.36	0.12	64	19	0.69
BFA-60/DMA-40/EDMA-1	0.65	0.21	101	12	0.87
EFA-20/DMA-80/EDMA-1	0.46	0.14	87	16	0.62
EFA-40/DMA-60/EDMA-1	0.59	0.18	97	15	0.72
EFA-60/DMA-40/EDMA-1	0.61	0.22	106	13	0.94
EFMA-20/DMA-80/EDMA-1	0.18	0.06	35	34	0.60
EFMA-40/DMA-60/EDMA-1	0.46	0.14	78	16	0.68
EFMA-60/DMA-40/EDMA-1	0.67	0.15	78	17	0.80
2 wt% EDMA					
BFA-20/DMA-80/EDMA-2	0.36	0.12	70	18	0.68
BFA-40/DMA-60/EDMA-2	0.65	0.21	108	11	0.75
BFA-60/DMA-40/EDMA-2	0.71	0.22	102	14	0.96
EFA-20/DMA-80/EDMA-2	0.34	0.11	60	21	0.68
EFA-40/DMA-60/EDMA-2	0.66	0.21	107	12	0.78
EFA-60/DMA-40/EDMA-2	1.35	0.45	209	7	0.98
EFMA-20/DMA-80/EDMA-2	0.73	0.23	131	9	0.66
EFMA-40/DMA-60/EDMA-2	0.82	0.26	134	10	0.74
EFMA-60/DMA-40/EDMA-2	1.22	0.39	185	8	0.95
5 wt% EDMA					
BFA-20/DMA-80/EDMA-5	1.19	0.31	164	31	0.74
BFA-40/DMA-60/EDMA-5	1.53	0.40	193	20	0.89
BFA-60/DMA-40/EDMA-5	1.09	0.35	161	9	1.06
EFA-20/DMA-80/EDMA-5	0.75	0.25	129	29	0.74
EFA-40/DMA-60/EDMA-5	1.44	0.37	181	28	0.83
EFA-60/DMA-40/EDMA-5	1.27	0.41	186	8	1.05
EFMA-20/DMA-80/EDMA-5	0.92	0.30	160	8	0.70
EFMA-40/DMA-60/EDMA-5	1.31	0.42	206	6	0.84
EFMA-60/DMA-40/EDMA-5	1.39	0.44	202	7	1.03

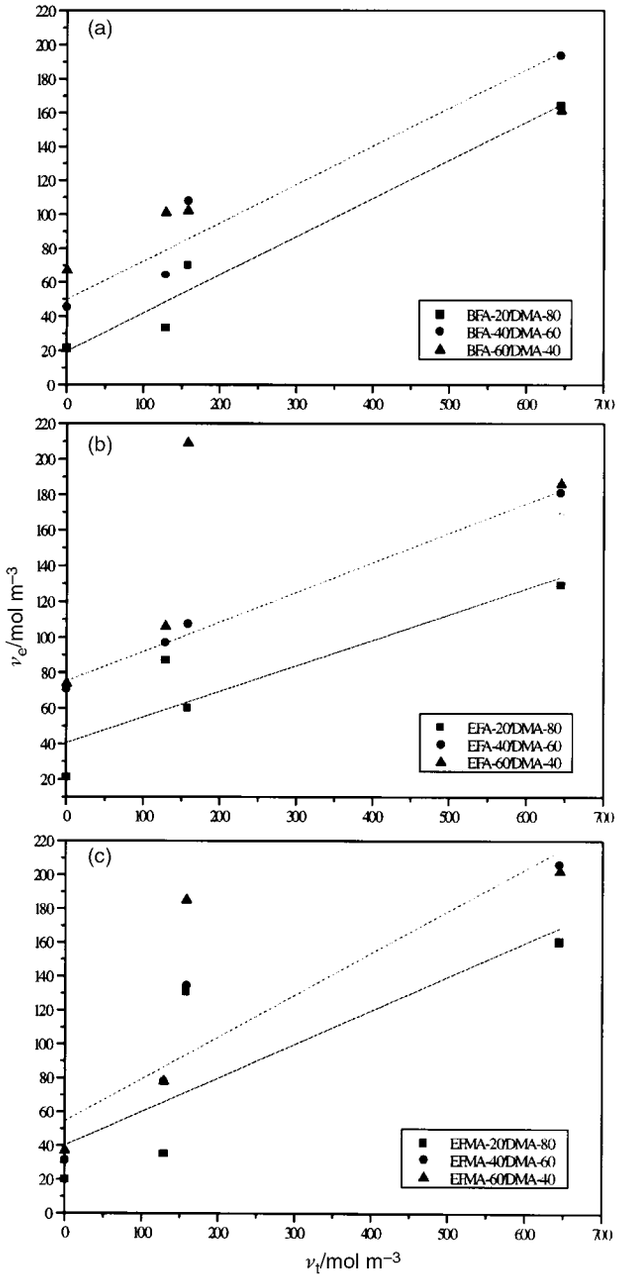

Fig. 5 Relationship between theoretical crosslinking density (v_t) and effective crosslinking density (v_e). (a) BFA/DMA, (b) EFA/DMA, (c) EFMA/DMA. ■ represents BFA, EFA or EFMA-20/DMA-80, ● BFA, EFA or EFMA-40/DMA-60 and ▲ BFA, EFA or EFMA-60/DMA-40. Lines of best fit were not taken for hydrogels containing 60 wt% fluoromonomer since they did not adhere to a linear relationship.

Table 7 Slopes and intercepts relating theoretical crosslinking density (v_t) and effective crosslinking density (v_e)

Material	Slope	Intercept
BFA-20/DMA-80 ■	0.22	20
BFA-40/DMA-60 ●	0.23	50
EFA-20/DMA-80 ■	0.14	41
EFA-40/DMA-60 ●	0.17	75
EFMA-20/DMA-80 ■	0.20	40
EFMA-40/DMA-60 ●	0.25	55

high oxygen permeabilities at high water contents and mechanical properties comparable with literature values given for existing contact lens materials.

Acknowledgements

3M Chemical Co. for generously donating the fluorinated monomers. CRC-ERT/CCLRU at UNSW for use of oxygen permeability testing equipment. Unisearch for generous funding and the granting of an Australian Postgraduate Award to Lisa Muratore.

References

1 O. Wichterle and D. Lim, *Nature (London)*, 1960, January 9, 117.
2 B. Tighe, *Optician*, 1989, June 2, 17.
3 B. Tighe, *Optician*, 1989, July 7, 17.
4 K. F. Mueller, US Pat., 5,011,275, 1991.
5 J. Salamone, US Pat., 4,990,582, 1991.
6 K. F. Mueller and W. L. Plankl, US Pat., 5,155,056, 1992.
7 J. J. Falcetta, US Pat., 4,640,965, 1987.
8 T. P. Davis, M. B. Huglin and D. C. F. Yip, *Polymer*, 1988, **29**, 701.
9 T. P. Davis and M. B. Huglin, *Macromolecules*, 1989, **22**, 2824.
10 T. P. Davis and M. B. Huglin, *Polymer*, 1990, **31**, 513.
11 T. P. Davis and M. B. Huglin, *Makromol. Chem.*, 1990, **191**, 331.
12 L. C. Winterton, J. C. White and K. C. Su, *Int. Contact Lens Clin.*, 1987, **14**(11), 441.
13 L. C. Winterton, J. C. White and K. C. Su, *Int. Contact Lens Clin.*, 1988, **15**(4), 117.
14 X. Xie and T. E. Hogen-Esch, *Macromolecules*, 1996, **29**, 1734.
15 Y. Liu, M. B. Huglin, R. Mao and P. A. Holmes, *Polymer*, 1996, **37**, 5069.
16 I. J. Park, S.-B. Lee and C. K. Choi, *Polymer*, 1997, **38**(10), 2523.

Paper a908656k